Discovery

To Cite:
Hezekiah-Braye O, Nonju GT. Sustainable synthetic fluid of Dehydration in Natural Gas Pipeline using Rubber Latex. *Discovery* 2026; 62: e24d3306
doi:

Author Affiliation:
[1]Department of Petroleum Engineering, Faculty of Engineering, P.M.B. 5080, Port Harcourt, Nigeria,
Email: oritom.hezekiah-braye1@ust.edu.ng
[2]Department of Petroleum Engineering, Faculty of Engineering, P.M.B. 5080, Port Harcourt, Nigeria,
Email: godloves.nonju@ust.edu.ng

Peer-Review History
Received: 16 September 2025
Reviewed & Revised: 07/October/2025 to 21/July/2026
Accepted: 03 August 2026
Published: 16 August 2026

Peer-Review Model
External peer-review was done through double-blind method.

Discovery
pISSN 2278–5469; eISSN 2278–5450

Sustainable synthetic fluid of Dehydration in Natural Gas Pipeline using Rubber Latex

Oritom Hezekiah-Braye[1], Godloves T Nonju[2]

ABSTRACT

Submarine developments significantly increase operational challenges related to intervention and flow assurance. In subsea pipelines, low seawater temperatures frequently induce gas hydrate formation. Using a 12-meter closed loop designed for hydrate research, this study investigated the impact of rubber latex on suppressing hydrate plug formation in gas-dominated systems. During testing, water and natural gas were circulated at 150 psi, utilizing 0.04 wt% and 0.05 wt% rubber latex as a kinetic inhibitor. Hydrates formed when 0.04 wt% rubber latex was used, causing the uninhibited system pressure to drop from 150 psi to 70 psi alongside visible hydrate clogging. Conversely, increasing the concentration to 0.05 wt% effectively kept the experimental loop free of hydrate plugs at 150 psi. Based on these experimental outcomes, mathematical models were developed to describe the performance of N-Vinylcaprolactam (N-VCap) within the system. Because inadequate chemical dosing can still allow hydrate formation under subsea conditions, field engineers must accurately determine effective inhibitor concentrations prior to operational deployment.

Keyword: Flow assurance, Rubber latex, Hydrate Inhibition, Subsea Pipelines, Kinetic Modeling

1. INTRODUCTION

Gas hydrate formation in production systems is particularly prevalent in challenging operational environments characterized by low temperatures, deep waters, and high water cuts (Bazvand et al., 2021). Under low temperatures and high pressures, water molecules react with light petroleum hydrocarbons—such as methane, ethane, propane, and butane—to form ice-like crystalline structures known as natural gas hydrates (Chatti et al., 2019). Non-hydrocarbon gases, including carbon dioxide, hydrogen sulfide, and nitrogen, can similarly trigger hydrate formation (Sloan et al., 2019). These formations pose severe operational challenges across the oil and gas sector (Giavarini et al., 2019). They can develop in wellbores during drilling following a gas kick or in reservoirs during carbon-dioxide-driven improved oil recovery (Grzelak et al., 2019). Hydrate plugs are well known for obstructing risers, chokes, blow-out preventers (BOPs), subsea transfer lines, and production pipelines (Stanek et al., 2019; Udachin et al., 2021). Additionally, permafrost regions naturally contain gas hydrate deposits (Sloan et al., 2019).

During drilling, gas released from natural hydrate deposits can migrate into the

wellbore, complicating well control and elevating disaster risks (Grzelak et al., 2019). Additional complications include flowline blockages, reduced gas throughput, steep system pressure drops, and downstream equipment damage caused by traveling hydrate debris (Hammerschmidt, 2020). Pipeline blockages can halt production entirely, leading to substantial financial losses as well as environmental and safety hazards. Hammerschmidt (1934) first documented hydrates in natural gas pipelines while inspecting a U.S. gas line, discovering that plugs previously assumed to be water ice were actually gas hydrates. This milestone highlighted the necessity of rigorous research into hydrate formation mechanisms and chemical prevention strategies (Javanmardian et al., 2019; Makogon, 2021).

Over the years, several operational strategies have been established to mitigate hydrate risks, primarily chemical treatment, phase separation, pressure management, and thermal control (Moon et al., 2022). Chemical inhibitors fall into two main categories: Thermodynamic Hydrate Inhibitors (THIs) and Low Dosage Hydrate Inhibitors (LDHIs) (Stanek et al., 2019). Polar compounds (such as alcohols and glycols) and ionic solutions (electrolytes) act as THIs; however, the corrosive nature of electrolytes limits their standalone application (Cha et al., 2019). Nevertheless, blending electrolyte solutions with glycols or alcohols reduces the total chemical volume needed. Research by Odutola et al. (2014) demonstrates that natural formation water salinity can act as an inherent inhibitor, reducing required THI volumes by approximately 14%.

Due to the significant capital and operational costs associated with storing and supplying THIs at onshore and offshore facilities, novel hydrate management strategies have gained traction (Okereke et al., 2019). Effectively implementing these strategies requires a thorough understanding of hydrate nucleation and growth dynamics (AlHarooni et al., 2019). Hydrate formation generally proceeds in two distinct steps: a nucleation phase requiring minimal gas consumption, followed by a rapid growth phase where hydrate particles form and agglomerate. The overall conversion rate of methane into hydrate crystals measures this formation pace (Gaillard et al., 1999).

According to Chittawan (2012), LDHIs are modern chemical compounds engineered to alter hydrate formation kinetics. They function at significantly lower concentrations than THIs, typically requiring less than 1–3 wt% in the aqueous phase. LDHIs are divided into two categories: Anti-Agglomerants (AAs) and Kinetic Hydrate Inhibitors (KHIs) (Davies et al., 2020). AAs are surface-active agents that disperse free water as tiny droplets within an entrained oil or condensate phase, preventing hydrate crystals from clumping together (Huo et al., 2021). KHIs are water-soluble polymers—frequently containing small cyclic amide groups—that delay crystal nucleation and early growth (Guan, 2010), granting production fluids sufficient residence time to pass through the pipeline without forming plugs. For KHIs to function effectively, the delivery system must maintain an active dosage throughout the fluid's pipeline residence time.

The development of KHIs was directly inspired by research on Ice-Structuring Proteins (ISPs) or anti-freeze proteins found in cold-adapted organisms, plants, fish, and insects. By binding to ice crystal nucleation sites, these proteins suppress ice growth and recrystallization, protecting the organism from freezing. In 1991, researchers at the Colorado School of Mines identified polyvinylpyrrolidone (PVP) as the first synthetic KHI (Kelland, 2022). Since then, various high-molecular-weight substances, including rubber latex derivatives, have been evaluated for KHI performance.

Rubber latex (containing active N-Vinylcaprolactam structures) acts as an anti-nucleation agent, interfering with structural crystal growth sites to prolong hydrate induction times. Evaluating KHI performance depends on defining key target conditions, particularly maximum water residence time and the expected degree of subcooling in the fluid stream (Sloan, 2023). Candidate KHIs must be validated in laboratory settings under representative fluid composition, pressure, and temperature conditions before field deployment (Brustad et al., 2020; Smelik et al., 2022; Talaghat, 2011). This study utilizes a laboratory micro flow loop to evaluate the performance of two distinct concentrations of rubber latex on gas hydrate suppression.

2. MATERIAL AND METHODS

To extend the exposure time of the fluid within the coldest zone, approximately 0.7 meters of the loop—configured in a spiral layout (Figure 1)—remains uninsulated inside the refrigeration unit. Because this section reaches the lowest temperatures, hydrate nucleation typically originates here. A dedicated test point connected via 1/4" tubing attaches to valve V5 off the spiral section (Figure 1). The overall skid-mounted flow loop includes three Atlas electrical pumps, a manual hydraulic pump, a refrigeration unit, two Rosemount differential pressure transmitters, a central control panel, a Madelena liquid flow meter, a gas flow meter, five temperature sensors, three pressure relief valves, eight pressure gauges, a gas mixing vessel, an inhibitor preparation vessel, and a compressed natural gas (CNG) cylinder.

Figure 1. Rubber Latex (Source: Julie-Anne et al., 2016)

The experimental focus centers on investigating hydrate formation kinetics within a laboratory micro flow loop (Figure 2). The setup consists of a 12-meter closed loop constructed from 0.5-inch internal diameter 316 stainless steel tubing. To maintain cooling, the steel line is encased inside a 4-inch polyvinyl chloride (PVC) jacket through which chilled water continuously circulates. During testing, the outer PVC jacket is insulated against ambient temperature fluctuations. Operating at pressures up to 3,500 psi and temperatures ranging from 0∘C to 50∘C, the system simulates subsea pipeline conditions cooled by surrounding ocean water.

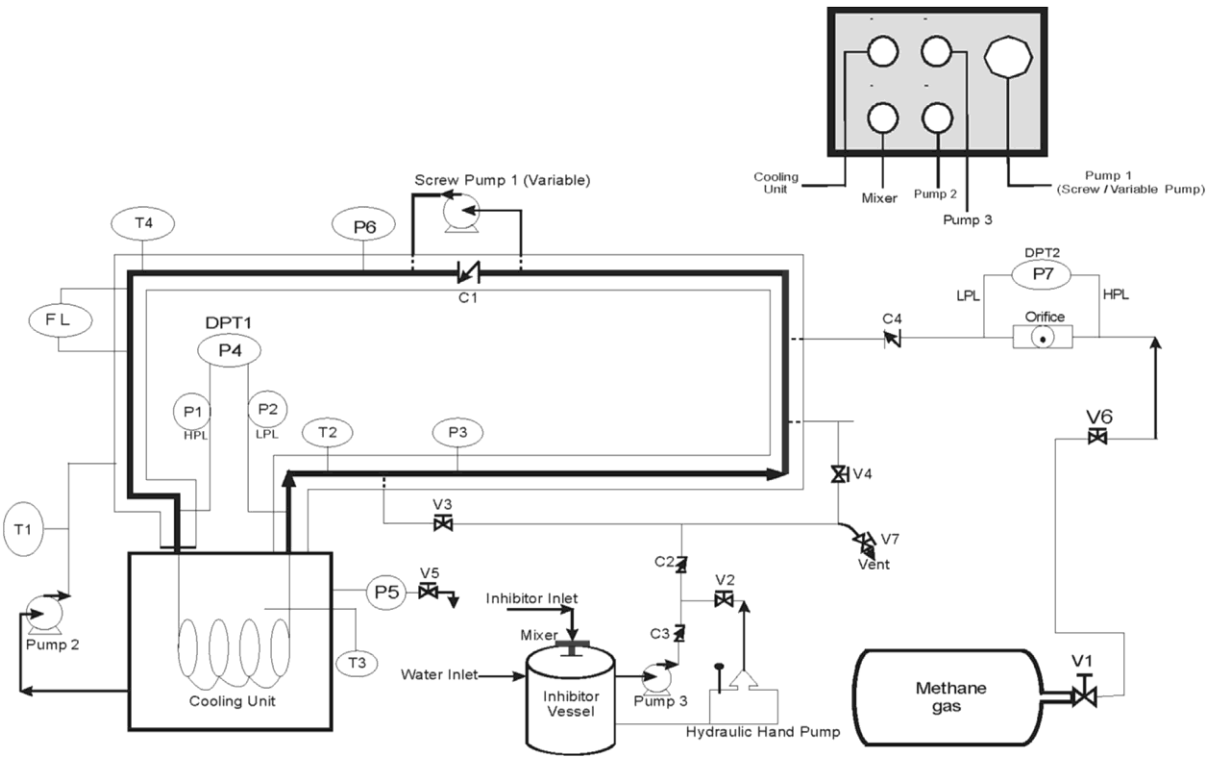

Figure 2. Diagram of a tiny flow loop in the lab for hydrate research

Experimental materials included water, ice for refrigeration, rubber latex as the kinetic inhibitor, and compressed natural gas containing over 98% methane. Baseline experiments were conducted by pressurizing water and natural gas inside the loop to 150 psi to establish uninhibited hydrate formation conditions. Pressure and temperature values were continuously logged as the system cooled toward hydrate formation thresholds.

During a standard run, water was introduced into the system from the supply vessel until system pressure reached 25 psi. Methane gas was then injected through the inlet orifice until system pressure stabilized at 150 psi. The variable-speed screw pump was engaged to establish a circulation velocity of 240 ft/h. Pump 2 was started to circulate chilled water from the refrigeration unit, with ice continuously added to accelerate thermal decline. Temperature and pressure readings were recorded at two-minute intervals throughout the two-hour test window. To evaluate chemical efficacy, identical procedures were repeated using aqueous solutions containing 0.04 wt% and 0.05 wt% rubber latex (N-Vinylcaprolactam).

Inhibitor performance was assessed based on the following thermodynamic criteria, where meeting any condition indicated inhibitor failure:

a. An abrupt temperature rise during the run, signaling an exothermic hydrate formation reaction.
b. A sudden spike in differential pressure between the inlet and outlet of the cooling unit, indicating hydrate accumulation along the pipe walls.
c. Blockage of the 1/4" tubing test port, as its narrow diameter makes it highly susceptible to plugging.

Visible hydrate crystals recovered in the effluent following system depressurization.

3. RESULTS & DISCUSSION

Differential pressure and system temperature were plotted against time for both uninhibited and chemical-treated systems. In the uninhibited run, differential pressure increased steadily over time (Figure 3). System temperature dropped consistently during the first 32 minutes; however, at minute 34, temperature spiked from 9∘C to 11∘C, confirming the onset of exothermic hydrate nucleation. The temperature subsequently dropped as heat from nucleation dissipated into the circulating coolant. By minute 67, temperature stabilized below 7∘C for roughly 19 minutes before a second exotherm occurred at minute 86. Following this second spike, temperatures rose steadily until the test concluded (Figure 3).

To describe this baseline behavior, a 10th-order polynomial thermodynamic model was developed, matching experimental observations closely (R2=0.99012; Figure 4).

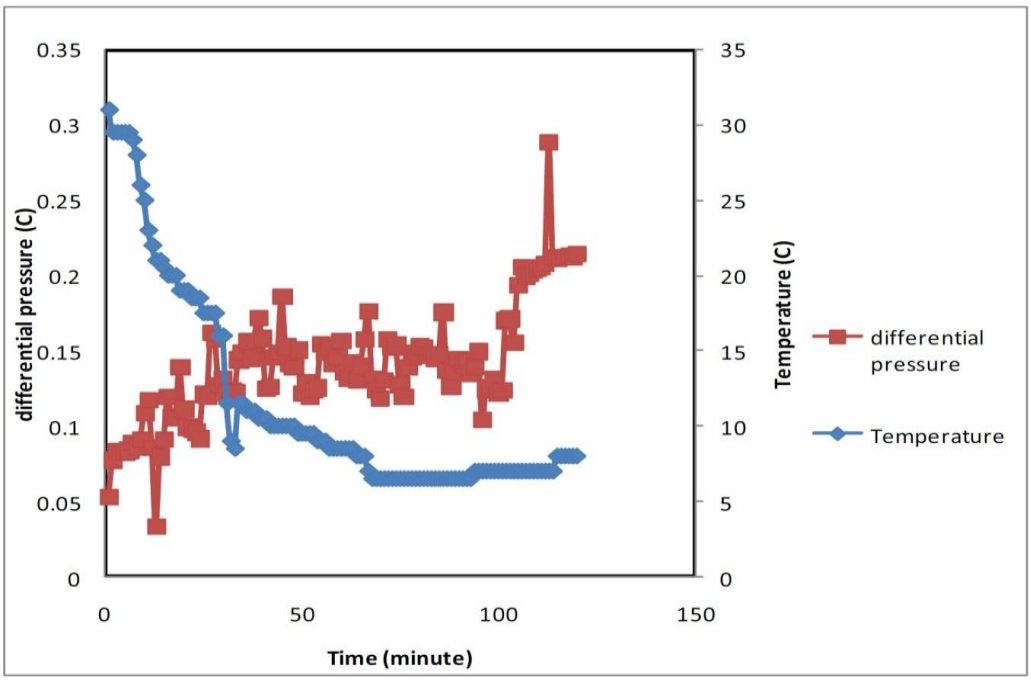

Figure 3. Temperature and differential pressure against time for an unrestricted system

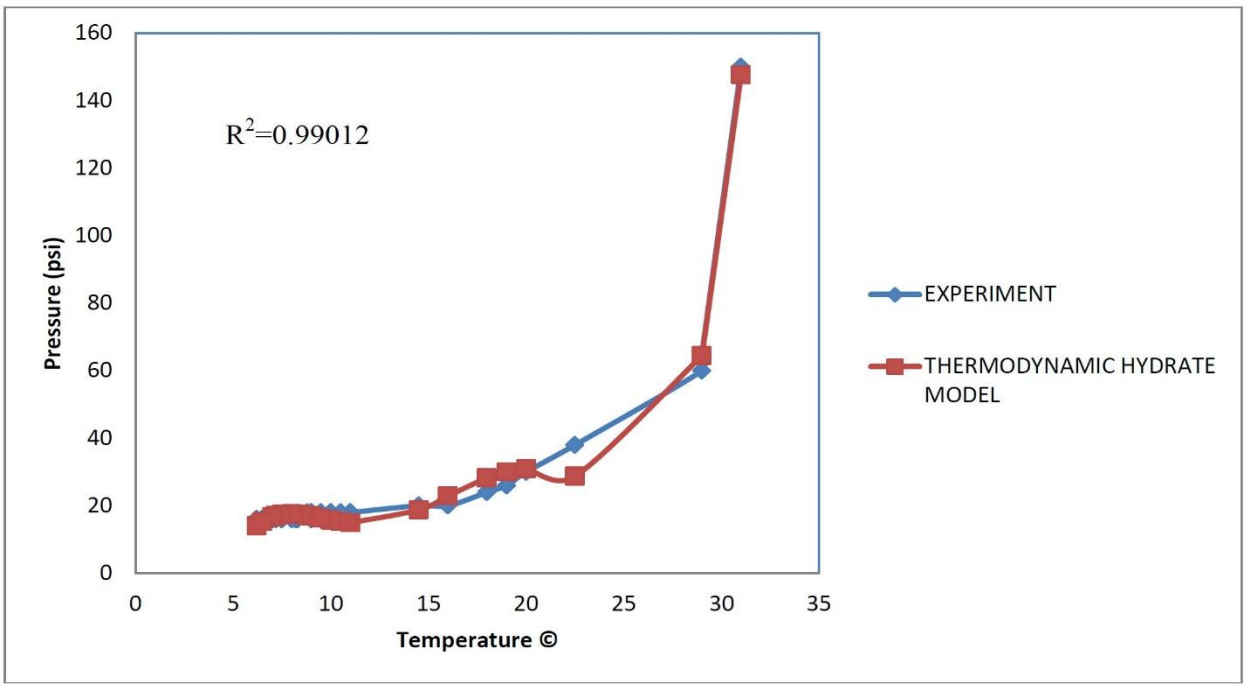

Figure 4. Plot illustrating the development of an experimental hydrate and the resultant hydrate model

$$P = 4.142 * 10^{-4}T^5 - 3.353 * 10^{-2}T^4 + 1.022T^3 - 14.502T^2 + 95.886T - 220.75 \quad (1)$$

P = Pressure (psi)

T = Temperature (°C)

For the run utilizing 0.04 wt% rubber latex (N-VCap), differential pressure trended downward for the first 24 minutes before oscillating near 0.32 bar, with no significant pressure spikes observed (Figure 5). System temperature dropped rapidly by 5∘C before slightly recovering to 7∘C at minute 54. After remaining at 7∘C for nearly 50 minutes, a minor increase to 7.5∘C was recorded. This indicates that while 0.04 wt% dosage delayed hydrate growth for approximately 50 minutes, it was insufficient to prevent hydrate formation across the full two-hour window. Because wall deposits were thin and did not restrict the effective internal diameter of the pipe, noticeable differential pressure spikes did not occur.

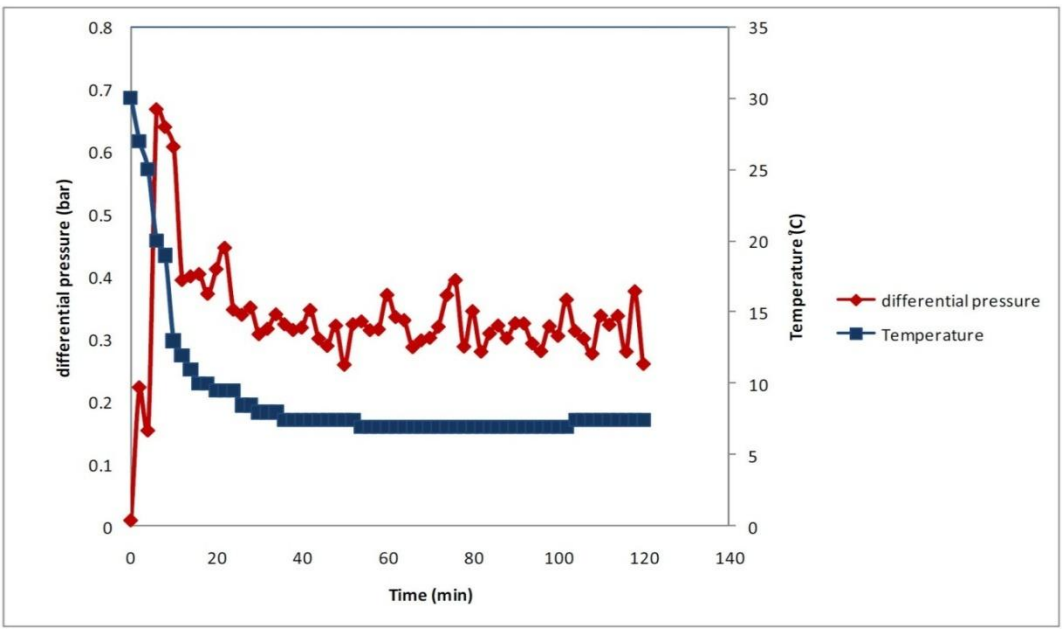

Figure 5. Temperature and pressure differentials against time for 0.04wt% N-VCap

In the test with 0.05 wt% N-VCap, differential pressure fluctuated minorly around 0.30 bar without significant spikes (Figure 6). System temperature fell sharply from 31.5∘C to 13∘C within 12 minutes, followed by a gradual decrease to 8∘C over the next 24 minutes. Thereafter, temperatures declined steadily to a final value of 6.5∘C with no exotherms detected. This confirms that a 0.05 wt% concentration effectively suppresses hydrate formation throughout the test duration.

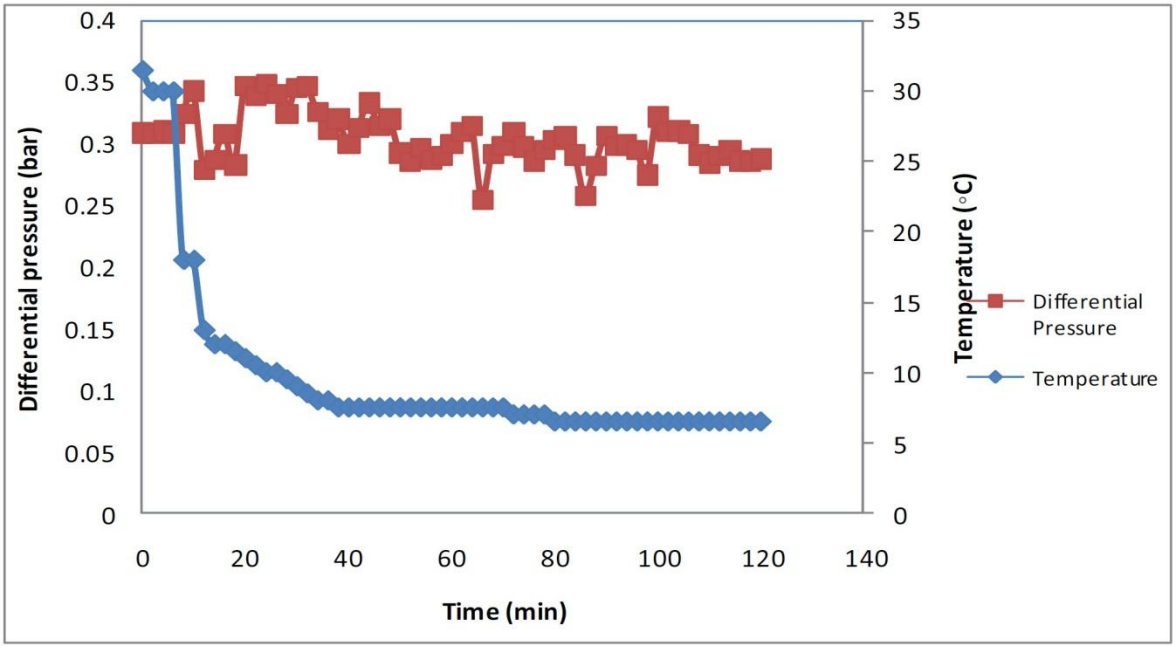

Figure 6. Temperature and differential pressure against time for 0.05wt% N-VCap

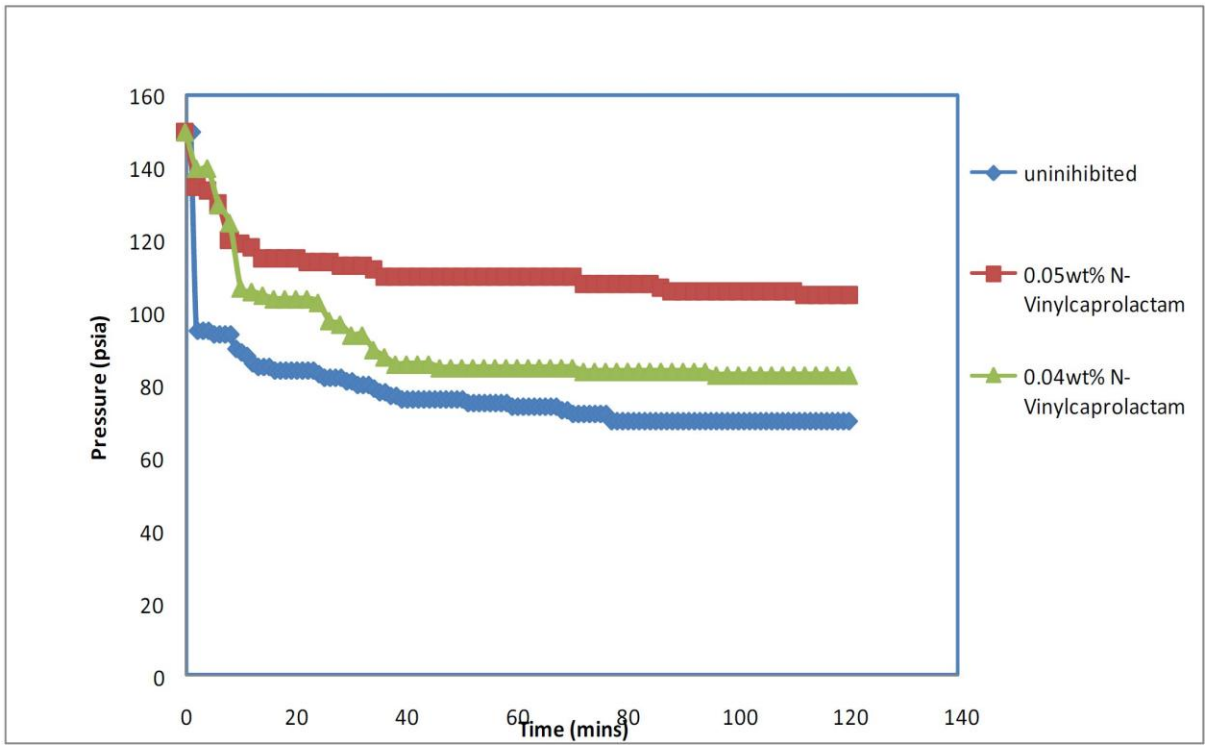

Figure 7. Pressure against time for the uncontrolled system and the 0.04wt% and 0.05wt% concentrations of N-VCap

To compare dosage performance, system pressure was tracked against time (Figure 7). Because testing was conducted in a closed batch system, pressure drops directly reflect gas consumption during hydrate growth. In the uninhibited run, system pressure fell from

150 psi to 70 psi over two hours, indicating significant gas conversion into hydrates (Figure 7). At 0.04 wt% concentration, pressure dropped from 150 psi to 83 psi, representing moderate hydrate growth. For the 0.05 wt% run, pressure dropped significantly less—from 150 psi to 105 psi. Although minor pressure decay occurred due to localized gas uptake, no significant exotherms or differential pressure spikes were detected because generated heat was rapidly dissipated by the cooling loop.

Equation 2 deduces a kinetic model for forecasting the pressure at which hydrates develop in the uncontrolled system.

$$P = 65.65 + \frac{519.95}{t} - \frac{3769.05}{t^2} + \frac{12504.05}{t^3} - \frac{18082.2}{t^4} + \frac{8911.19}{t^5} \quad (2)$$

Additionally, kinetic models were generated to estimate pressure when the inhibitor was 0.04 weight percent N-VCap (equation 3) or 0.05 weight percent N-VCap (equation 4).

$$P = -2.456 * 10^{-8}t^5 + 9.395 * 10^{-6}t^4 - 1.403 * 10^{-3}t^3 + 0.104t^2 - 3.981t + 148.55 \quad (3)$$
$$P = -4.113 * 10^{-8}t^5 + 1.446 * 10^{-5}t^4 - 1.901 * 10^{-3}t^3 + 0.115t^2 - 3.204t + 144 \quad (4)$$

P = Pressure in psi

t = Time in minutes

4. CONCLUSION

Rubber latex serves as an effective kinetic hydrate inhibitor, capable of delaying nucleation and growth to ensure plug-free pipeline operations. Prior to field application, representative fluid samples must be evaluated across various concentrations to determine optimum chemical dosing. Micro flow loop testing provides a reliable platform for evaluating minimum effective dosage based on field residence times. In this work, thermodynamic and kinetic models were successfully established to model system pressure variations and evaluate N-VCap performance.

Acknowledgement

Our profound gratitude is to our beloved ones for their immeasurable support and to Mr. Edmund Obi for his honourable support and prayers.

Author Contributions

Oritom Hezekiah-Braye: Conceptualization, methodology, experimental design, laboratory investigation, data analysis, interpretation of results, manuscript drafting, and supervision.
Godloves T. Nonju: Experimental investigation, data collection, statistical analysis, literature review, manuscript preparation, editing, and revision.
Both authors read and approved the final version of the manuscript.

Informed consent

Not applicable.

Conflicts of interests

The authors declare that they have no conflicts of interest, competing financial interests or personal relationships that could have influenced the work reported in this paper.

Ethical approval & declaration

Not applicable. This article does not contain any studies with human participants or animals performed by any of the authors.

Funding

This research did not receive any external funding like specific grant from funding agencies in the public, commercial, or nonprofit sectors.

Data and materials availability

All data generated and analysed during this study are presented within this manuscript. Additional information supporting the findings of this study will be made available by the corresponding author upon reasonable request.

REFERENCES

1. AlHarooni K, Pack D, Iglauer S, Gubner R, Ghodkay V, Barifcani A. Analytical techniques for analyzing thermally degraded monoethylene glycol with methyl diethanolamine and film formation corrosion inhibitor. Energy Fuels 2019;30(11):10937-10949. doi: 10.1021/acs.energyfuels.6b02116
2. Bazvand M, Mahmudi S, Shabibi M. A new inhibitor to prevent hydrate formation. Pet Petrochem Eng J 2021;5(1):1-6. doi: 10.23880/ppej-16000252
3. Brustad S, Løken KP, Waalmann JG. Hydrate prevention using MEG instead of MeOH: Impact of experience from major Norwegian developments on technology selection for injection and recovery of MEG. Offshore Technology Conference 2020. doi: 10.4043/17453-MS
4. Cha M, Shin K, Kim J, Chang D, Seo Y, Lee H, Kang SP. Thermodynamic and kinetic hydrate inhibition performance of aqueous ethylene glycol solutions for natural gas. Chem Eng Sci 2019;99:184-190. doi: 10.1016/j.ces.2013.06.002
5. Chatti I, Delahaye A, Fournaison L, Petitet JP. Benefits and drawbacks of clathrate hydrates: A review of their areas of interest. Energy Convers Manag 2019;46(9-10):1333-1343. doi: 10.1016/j.enconman.2004.06.032
6. Chittawan N. Gas Hydrate Formation and Control by the Use of Chemicals (Master's thesis). University of Stavanger 2012.
7. Davies L, Bollavaram P, Peters DJ. Hydrate plug dissociation. AIChE J 2020;52(12):4016-4027. doi: 10.1002/aic.10986
8. Gaillard C, Monfort JP, Peytavy JL. Investigation of methane hydrate formation in a recirculating flow loop: Modeling of the kinetics and tests of efficiency of chemical additives on hydrate inhibition. Oil Gas Sci Technol 1999;54(3):365-374. doi: 10.2516/ogst:1999032
9. Giavarini C, Hester K. Gas Hydrates: Immense Energy Potential and Environmental Challenges. Springer Science & Business Media 2019.
10. Grzelak H, Stenhaug T. Scale inhibition in wellbores. University of Tulsa Centennial Petroleum Engineering Symposium 2019. doi: 10.2118/27980-MS
11. Guan H. The inhibition of gas hydrates and synergy of the inhibiting molecules. International Oil and Gas Conference and Exhibition in China 2010. doi: 10.2118/131314-MS
12. Hammerschmidt EG. Formation of gas hydrates in natural gas transmission lines. Ind Eng Chem 1934;26(8):851-855. doi: 10.1021/ie50296a010
13. Hammerschmidt P. Experimental thermodynamic parameters for the prediction of natural gas hydrate dissociation conditions. Ind Eng Chem Fundam 2020;19(4):410-414. doi: 10.1021/i160076a018
14. Huo Z, Freer E, Lamar M, Sannigrahi B, Knauss DM, Sloan ED. Hydrate plug prevention by anti-agglomeration. Chem Eng Sci 2021;56(16):4979-4991. doi: 10.1016/S0009-2509(01)00139-2
15. Javanmardian R, Peytavy JL, Glénat P, Pou TE, Hidalgo M, Dicharry C. Laboratory evaluation of kinetic hydrate inhibitors: A procedure for enhancing the repeatability of test results. Energy Fuels 2019;23(2):962-966. doi: 10.1021/ef800806z
16. Kelland MA. History of the development of low dosage hydrate inhibitors. Energy Fuels 2022;20(3):825-847. doi: 10.1021/ef050427x
17. Makogon YF. A gas hydrate formation in the gas saturated layers under low temperature. Gas Ind 2021;5:14-15.
18. Moon C, Taylor PC, Rodger PM. Molecular dynamics study of gas hydrate formation. J Am Chem Soc 2022;125(16):4706-4707. doi: 10.1021/ja028537v
19. Odutola TO, Ikiensikimama SS, Dulu A. Chemical compromise: A thermodynamic and ionic solution to hydrate inhibition. SPE Nigeria Annual International Conference and Exhibition 2014. doi: 10.2118/172410-MS
20. Okereke NU, Edet PE, Baba YD, Izuwa NC, Kanshio S, Nwogu N, Afolabi FA, Nwanwe O. An assessment of hydrates inhibition in deepwater production systems using low-dosage hydrate inhibitor and monoethylene glycol. J Pet Explor Prod Technol 2019;10(3):1169-1182. doi: 10.1007/s13202-019-00812-w
21. Sloan ED, Koh CA. Clathrate Hydrates of Natural Gases. 3rd ed. CRC Press 2023.
22. Sloan ED, Koh CA. Quantifying hydrate formation and kinetic inhibition. Ind Eng Chem Res 2019;37(8):3124-3132. doi: 10.1021/ie9709593

23. Smelik EA, King HE. Crystal-growth studies of natural gas clathrate hydrates using a pressurized optical cell. Am Mineral 2022;82(1-2):88-98. doi: 10.2138/am-1997-1-210
24. Stanek WE, Białecki R. Thermodynamic model for predicting phase equilibria of simple clathrate hydrates of refrigerants. Chem Eng Sci 2019;66(21):5439-5445. doi: 10.1016/j.ces.2011.07.039
25. Talaghat MR. Experimental investigation of induction time for binary mixtures during gas hydrate. J Nat Gas Sci Eng 2011;3(6):715-718. doi: 10.1016/j.jngse.2011.08.002
26. Udachin KA, Ratcliffe CI, Ripmeester JA. Structure, composition, and thermal expansion of CO2 hydrate from single crystal X-ray diffraction measurements. J Phys Chem B 2021;105(19):4200-4204. doi: 10.1021/jp0043899